AIP | Physics of Fluids

Wall-modeling in large eddy simulation: Length scales, grid resolution, and accuracy

Soshi Kawai and Johan Larsson

Citation: Physics of Fluids (1994-present) **24**, 015105 (2012); doi: 10.1063/1.3678331
View online: http://dx.doi.org/10.1063/1.3678331
View Table of Contents: http://scitation.aip.org/content/aip/journal/pof2/24/1?ver=pdfcov
Published by the AIP Publishing

Wall-modeling in large eddy simulation: Length scales, grid resolution, and accuracy

Soshi Kawai[1,a)] and Johan Larsson[2]
[1]*Institute of Space and Astronautical Science, Japan Aerospace Exploration Agency, 3-1-1 Yoshinodai, Chuoku, Sagamihara, Kanagawa 252-5210, Japan*
[2]*Center for Turbulence Research, Stanford University, 488 Escondido Mall, Stanford, California 94305-3035, USA*

(Received 14 November 2011; accepted 2 December 2011; published online 31 January 2012)

This paper addresses one of the most persistent errors in wall-modeled large eddy simulation: the inevitable presence of numerical and subgrid modeling errors in the first few grid points off the wall, which leads to the so-called "log-layer mismatch" with its associated 10-15% error in the predicted skin friction. By considering the behavior of turbulence length scales near a wall, the source of these errors is analyzed, and a method that allows for the log-layer mismatch to be removed, thereby yielding accurately predicted skin friction, is proposed. © *2012 American Institute of Physics*. [doi:10.1063/1.3678331]

I. INTRODUCTION

When applied to turbulent boundary layers at high Reynolds numbers, the computational cost of large eddy simulation (LES) becomes highly prohibitive. Boundary layers are multi-scale phenomena where the energetic and dynamically important motions in the inner layer (say, the innermost 10% of the boundary layer) become progressively smaller in size as the Reynolds number increases, while the size of energetic motions in the outer layer is nearly independent of Reynolds number. If these inner-layer motions are resolved, the required grid resolution necessarily scales with the viscous length scale. Therefore, in order to make LES applicable to high Reynolds number wall-bounded flows, the inner layer must be modeled while directly resolving only the outer layer.

Let us consider what should be expected of a wall-modeled LES calculation. While clearly problem-specific, a reasonable requirement is to predict, for an equilibrium boundary layer: (1) accurate skin friction (for a given free-stream velocity) and (2) accurate turbulence (structure and statistics) in the LES region (i.e., the outer layer of the boundary layer). The first requirement is the most basic and rudimentary requirement on wall-modeled LES and equivalent to having an accurate ratio between the free-stream U_∞ and the wall friction velocity $u_\tau \equiv (\tau_w/\rho_w)^{1/2}$, where τ_w and ρ_w are the shear stress and the density at the wall. The importance of predicting skin friction accurately goes beyond simply getting the correct integral quantity for a flat plate. Consider an airfoil with flow separation: the exact point of separation (that directly affects the aerodynamic performance) will depend on the state of the upstream boundary layer, which will only be correct if the upstream skin friction was predicted accurately.

There have been many proposed methods for modeling of the inner layer in LES (cf. the reviews by Piomelli and Balaras[1] and Spalart[2]). These approaches generally fall into one of two categories: (1) methods that model the wall shear stress τ_w directly and (2) methods that switch to a Reynolds-averaged Navier-Stokes (RANS) description in the inner layer. The second category includes hybrid LES/RANS and detached eddy simulation (DES).

Generally speaking, models from both categories are capable of predicting the skin friction in a canonical boundary layer (or channel flow) to within 5%–15%, but a very persistent so-called "log-layer mismatch" plagues most methods and prevents more accurate skin friction predictions.

[a)]Author to whom correspondence should be addressed. Electronic mail: kawai@flab.isas.jaxa.jp.

Nikitin *et al.*[3] showed this clearly for DES, while others have shown it for different hybrid LES/RANS models.[4] While stochastic forcing[5] or other means[6,7] of stimulating turbulence can remove the log-layer mismatch, some studies (cf. Ref. 4) have found a range of possible log-law intercepts (or predicted skin friction coefficients) depending on the amplitude of the forcing. The cause of the log-layer mismatch is different in models from the wall-stress category but is, nevertheless, present in most studies. For example, Cabot and Moin[8] found a negative mismatch, while the present study finds a positive one. The purpose of the present study is to diagnose this problem in the context of wall-stress models and to propose a solution that allows for the log-layer mismatch to be removed.

In the wall-stress modeling approach,[8–10] the LES is formally defined as extending all the way down to the wall but is solved on a grid that only resolves the outer layer motions. A wall-model takes as input the instantaneous LES solution at a height $y=h_{\mathrm{wm}}$ above the wall and estimates the instantaneous shear stress τ_w at the wall $y=0$; this is then given back to the LES as a boundary condition. The natural choice, and the choice made in all prior studies to our knowledge, is to take the LES solution in the first grid point off the wall as input to the wall-model. The wall-model itself is generally based on RANS concepts of differing fidelities (e.g., with[9] or without[10] equilibrium assumptions).

Errors in wall-modeling can be categorized into two categories: (1) errors in the wall-model itself and (2) errors in the LES in the first few grid points off the wall. The focus of this study is on the second type of error, which exists regardless of the exact details of the wall-model itself. This error stems from the fact that the LES is necessarily underresolved in the first few grid points (to be discussed below), and hence, numerical and subgrid modeling errors cannot be avoided there. This argument was given by Cabot and Moin[8] and was given as a major reason by Nicoud *et al.*[11] for developing a wall-model based on control theory. In fact, the idea that numerical and modeling errors are unavoidable in the first few grid points and, crucially, the idea that these errors necessarily lead to errors in the computed flow field (e.g., the computed skin friction) is now broadly agreed upon in the wall-modeling community (cf. Pantano *et al.*[12]).

The source of this error is analyzed below, which leads directly to a proposal of a simple yet effective method to remove the impact of the error on the computed turbulence. The analysis and developments are presented for compressible flows, but everything extends trivially to incompressible flows. The proposed method allows for grid convergence (of statistics) by fixing the key wall-modeling parameter under grid refinement.

II. METHODOLOGY

A. Inner layer wall-model

Consider an LES mesh designed to resolve only the large scales in the outer layer (i.e., with grid resolution scaling with the boundary layer thickness δ). Assuming equilibrium, the unresolved inner layer is modeled by solving

$$\frac{d}{dy}\left[(\mu+\mu_{t,\mathrm{wm}})\frac{dU_{\|}}{dy}\right]=0,\quad \frac{d}{dy}\left[(\mu+\mu_{t,\mathrm{wm}})U_{\|}\frac{dU_{\|}}{dy}+c_p\left(\frac{\mu}{Pr}+\frac{\mu_{t,\mathrm{wm}}}{Pr_{t,\mathrm{wm}}}\right)\frac{dT}{dy}\right]=0, \tag{1}$$

in an overlapping layer between $y=0$ and $y=h_{\mathrm{wm}}$. The wall-model eddy viscosity is taken from the mixing length formula,

$$\mu_{t,\mathrm{wm}}=\kappa\rho y\sqrt{\frac{\tau_w}{\rho}}\mathcal{D},\quad \mathcal{D}=[1-\exp(-y^+/A^+)]^2,$$

with $\kappa=0.41$, $Pr_{t,\mathrm{wm}}=0.9$, and $A^+=17$. The boundary condition at $y=0$ for Eq. (1) is the adiabatic (or isothermal) no-slip condition; at $y=h_{\mathrm{wm}}$, the wall-parallel velocity $U_{\|}$ and the temperature T are imposed from the instantaneous LES solution. After solving the system of two coupled ordinary differential equations (ODEs) (1), the shear stress τ_w and the heat flux q_w at the wall can be directly computed and fed back to the LES as a boundary condition at the wall. Note that the pressure is constant in the wall-normal direction and simply imposed by the LES solution at

$y = h_{\rm wm}$, and also that Eq. (1) is equivalent to the famous log-law in the inviscid region in the limit of incompressible flow without heat transfer.

B. Outer layer LES method

The dynamic Smagorinsky model of Moin *et al.*[13] with the modification of Lilly[14] with averaging in the spanwise (homogeneous) direction is used to calculate the turbulent eddy viscosity $\mu_{\rm sgs}$ and turbulent Prandtl number $Pr_{\rm sgs.}$ At walls, the kinematic no-penetration condition implies that the convective terms are zero. In addition, the viscous work term $\tau_{ij}u_i$ is zero at the wall due to the no-slip condition (the fact that the LES does not resolve the inner layer does not change the fact that $u_i = 0$ at a wall, only that the gradient cannot be computed accurately).

The numerical method is fully conservative and uses a sixth-order compact differencing scheme[15] in space and fourth-order Runge-Kutta integration in time. Aliasing errors are contained by applying an eighth-order low-pass filter[15,16] to the conserved variables at regular intervals. The code has been extensively verified and validated.[17–20] The fact that the viscous inner layer is not resolved implies that some changes are needed in the numerical method. Simply put, differentiation and filtering between points above and below the missing inner layer (i.e., between the first grid point at $j = 1$ and the wall at $j = 0$) are ill-defined and inaccurate. We instead compute wall-normal derivatives used in the viscous fluxes at $j = 1$ using a completely one-sided formula and at $j = 2$ using a second-order central formula; remaining grid points are treated by the tri-diagonal compact scheme. Although, given these numerical treatments, the LES equations can be evaluated without specifying the velocities, density, and temperature at the wall, we use slip-wall conditions with extrapolation from the interior nodes to calculate the dynamic Smagorinsky model and for low-pass spatial filtering.

The computational domain for the wall-modeled LES is $15\delta_r$, $15\delta_r$, and $3\delta_r$ in the streamwise (x), wall-normal (y), and spanwise (z) directions, where δ_r is a reference boundary layer thickness that is close to its value at the inlet. The wall is located at $y = 0$, and the corresponding grid index is $j = 0$, hence $y_0 = y_w = 0$. The boundary layer thickness δ at the station where statistics are compared is $\delta \approx 1.2\delta_r$ ($x \approx 12\delta_r$). A buffer layer with the length of $12\delta_r$ is placed at the upper boundary to remove reflections from the boundary. The rescaling-reintroducing method of Urbin and Knight[21] is used to produce realistic turbulence at the inflow with the recycling station taken as $12\delta_r$ downstream of the inflow. The present computational domain size and the location at which the data is extracted were found to be sufficient to not affect the turbulence statistics in a prior study.[22]

III. ERRORS IN THE NEAR-WALL GRID POINTS IN THE LES

Having introduced the wall-modeled LES framework, we next discuss the numerical and subgrid-modeling errors in the first few grid points off the wall. The key point about this type of error is that it persists even with a "perfect" wall-model (i.e., perfectly estimated τ_w).

Consider LES of a boundary layer of thickness δ at high Reynolds number. A wall-model models the processes between the wall and a location $y = h_{\rm wm}$ (which is typically taken as the first grid point off the wall, i.e., $h_{\rm wm} = y_1$). The height $h_{\rm wm}$ should be fixed in outer units in order to lead to a computational cost that is nearly independent of Reynolds number. Moreover, since the classic picture of a boundary layer (cf. Ref. 23) suggests that the inner layer $y \lesssim 0.1\delta$ is to some degree universal with minimal influence from the free-stream, it follows that $h_{\rm wm} \approx 0.1\delta$ is a good choice. In the analysis, let us also assume that the first grid point is located in the (inviscid) log-layer, i.e., that $y_1^+ \gtrsim 50$. This assumption simplifies the analysis and is reasonable for wall-modeled LES at high Reynolds numbers. Using only conservation of momentum, it is easy to derive the average shear-stress balance in the log-layer (i.e., $50 \lesssim y^+ \lesssim 0.1\delta^+$) as

$$\bar{\mu}_{\rm sgs}\partial_y\tilde{u} - \bar{\rho}\widetilde{u''v''} = \tau_w, \tag{2}$$

which shows that the mean velocity gradient is a result of a balance between the total shear stress τ_w, the resolved shear stress $-\bar{\rho}\widetilde{u''v''}$, and the average subgrid eddy-viscosity $\bar{\mu}_{\rm sgs}$.

The size of the energetic and stress-carrying motions in the log-layer is proportional to the wall-distance y (cf. Ref. 23). It is reasonable to assume different sizes in the different directions, and hence, one can take the length scale of the stress-carrying motions as $L_i = C_i y$, where C_i is a (different) constant for each direction i. To resolve motions of size L_i accurately, a grid-spacing $\Delta x_i \lesssim L_i/N$ is needed, where the value of N (i.e., the number of grid points per wavelength) depends on the particular numerical method used for the LES. Thus, the stress-carrying motions are properly resolved at height y only if

$$\frac{\Delta x_i}{y} \lesssim \frac{C_i}{N}, i = 1, 2, 3. \tag{3}$$

Consider a uniform grid with $y_j = j\Delta y$. The standard approach is to estimate the wall-stress (and wall heat flux) by solving the wall-model between the wall ($y = 0$) and the first grid point (i.e., to use $h_{\mathrm{wm}} = y_1$). The criterion (3) in the $i = 2$ direction implies that the stress-carrying motions at height $y = y_1 = \Delta y$ in the LES are accurate only if $C_2 \gtrsim N$. This is highly unlikely: the numerical Nyquist criterion implies $N \geq 2$, and the kinematic damping by the wall makes $C_2 \lesssim 2$ a very reasonable upper bound. Hence, the LES is necessarily underresolved at the first grid point y_1. Since the wall-model in all prior studies (to our knowledge) has taken as input the instantaneous solution from the LES at the first grid point, it is clear that the wall-model has been fed underresolved and thus inaccurate information. Therefore, even a perfect wall-model would not be able to accurately predict the skin friction (when the wall-model is applied between the first grid point y_1 and the wall).

A. Proposed improvement

The reasoning up to this point is simply a repeat of the arguments given by Cabot and Moin,[8] Nicoud *et al.*,[11] and others to argue that wall-models are unavoidably affected by numerical and subgrid modeling errors, but from here on, we depart in a different direction. The crucial point in the proposed method is to realize that there is nothing requiring the wall-model to be applied between the first grid point y_1 and the wall: the wall-model equations are valid for *any* interval from the wall and up (provided the upper point is within the inner portion of the boundary layer). Let us allow $h_{\mathrm{wm}} \neq y_1$ (i.e., $h_{\mathrm{wm}} = y_j$, $j \geq 1$), the criterion (3) then yields that the LES is properly resolved at $y = h_{\mathrm{wm}}$ only if

$$\frac{\Delta x_i}{h_{\mathrm{wm}}} \lesssim \frac{C_i}{N}, \; i = 1, 2, 3.$$

In the wall-parallel and wall-normal directions, this becomes

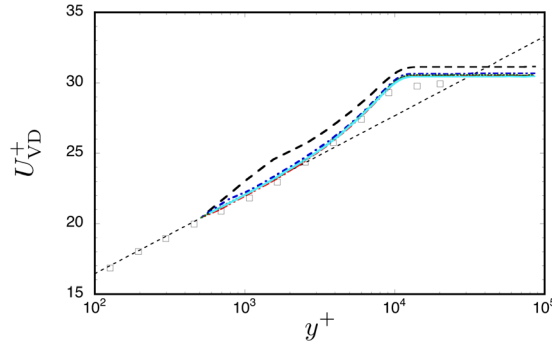

FIG. 1. (Color online) Mean velocity (van Driest-transformed) at $Re_\delta = 6.1 \times 10^5$ ($Re_\theta = 5 \times 10^4$) compared to the log-law $\ln(y^+)/0.41 + 5.2$ (thin dashed line, black) and incompressible experiments at $Re_\theta = 3.1 \times 10^4$ (squares[27]). Fixed $h_{\mathrm{wm}}/\delta = 0.055$ and $\Delta x/\delta = \Delta z/\delta = 0.042$. Varying $\Delta y_w/h_{\mathrm{wm}}$ of 1.0 (dashed line, black), 0.50 (dashed-dotted line, blue), 0.33 (double-dashed double-dotted line, red), 0.25 (dotted line, green), and 0.20 (solid line, cyan).

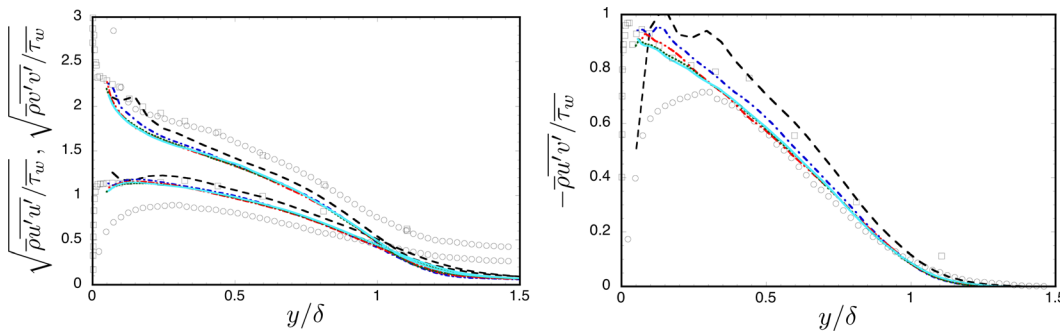

FIG. 2. (Color online) Resolved Reynolds normal stresses (left) and shear stress (right) at $Re_\delta = 6.1 \times 10^5$ ($Re_\theta = 5 \times 10^4$). Fixed $h_{\rm wm}/\delta = 0.055$ and $\Delta x/\delta = \Delta\, z/\delta = 0.042$. Varying $\Delta y_w/h_{\rm wm}$ as in Fig. 1 compared to corresponding experiments (circles[25,26]) and incompressible experiments at $Re_\theta = 1.3 \times 10^4$ (squares[27]).

$$\frac{\Delta x_{1,3}}{h_{\rm wm}} \lesssim \frac{C_{1,3}}{N}, \tag{4a}$$

$$\frac{\Delta y}{h_{\rm wm}} \lesssim \frac{C_2}{N}, \tag{4b}$$

respectively. The value of N is related to the numerical method while the values of C_i are dictated by flow physics, specifically the structure and size of the energetic motions in the log-layer.

Note that the criterion (4b) in the wall-normal direction is closely related (in spirit) to the technique of explicitly filtered LES;[24] one should choose the height $h_{\rm wm}$ of the wall-modeling layer based on flow physics and then refine the grid *without changing this height* until numerical and subgrid modeling errors have been made negligibly small at $y = h_{\rm wm}$. This can only be achieved by abandoning the established practice of applying the wall-model between the first grid point off the wall (at y_1) and the wall itself.

We emphasize the overall reasoning here that the wall-model can only be expected to function properly if fed accurate information from the LES, which in turn implies that the LES must be well resolved at the point $h_{\rm wm}$ where information is fed into the wall-model. We next turn to numerical experiments to verify this argument.

B. Numerical experiments

The supersonic flat plate boundary layer experiment by Souverein *et al.*[25,26] is considered to verify the proposed idea. The free-stream Mach number is 1.69, and the Reynolds number is $Re_\delta = 6.1 \times 10^5$ ($Re_\theta = 5 \times 10^4$). We emphasize that this is a *much* higher Reynolds number than what traditional wall-resolved LES is capable of computing. Also, note that a subset of these

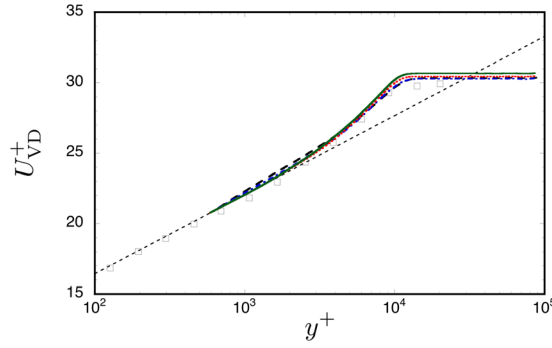

FIG. 3. (Color online) Mean velocity (van Driest-transformed) at $Re_\delta = 6.1 \times 10^5$ ($Re_\theta = 5 \times 10^4$) compared to the log-law $\ln(y^+)/0.41 + 5.2$ (thin dashed line, black) and incompressible experiments at $Re_\theta = 3.1 \times 10^4$ (squares[27]). Fixed $h_{\rm wm}/\delta = 0.055$ and $\Delta y_w/h_{\rm wm} = 0.20$. Varying $\Delta x/\delta = \Delta\, z/\delta$ of 0.084 (dashed line, black), 0.064 (dashed-dotted line, blue), 0.042 (dotted line, red), and 0.028 (solid line, green).

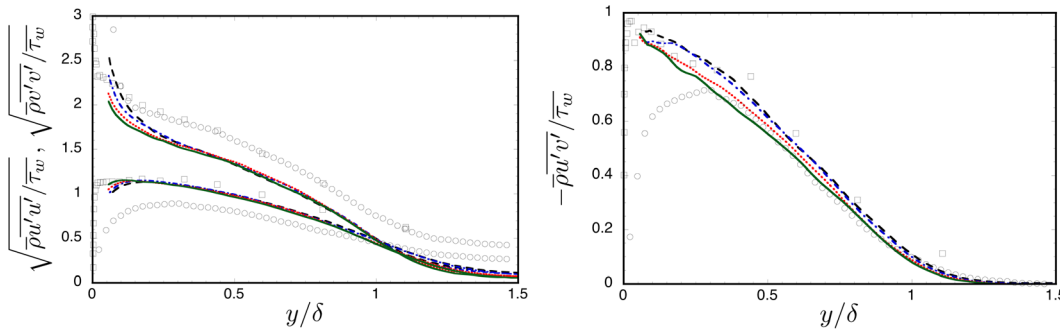

FIG. 4. (Color online) Resolved Reynolds normal stresses (left) and shear stress (right) at $Re_\delta = 6.1 \times 10^5$ ($Re_\theta = 5 \times 10^4$). Fixed $h_{\rm wm}/\delta = 0.055$ and $\Delta y_w/h_{\rm wm} = 0.20$. Varying $\Delta x/\delta$ and $\Delta z/\delta$ as in Fig. 3 compared to corresponding experiments (circles[25,26]) and incompressible experiments at $Re_\theta = 1.3 \times 10^4$ (squares[27]).

numerical tests was performed with a different code with very different numerical characteristics (non-dissipative through use of split-form derivatives), with the same convergence trends but at different critical values of the parameters C_i/N. Thus, the conclusions reached here are dependent on the numerics only insofar as exact numerical values of the parameters are concerned but not in the larger qualitative sense.

The first test investigates criterion (4b) on the wall-normal grid spacing. The height of the wall-layer is fixed at $h_{\rm wm} = 0.055\delta$. The grids have fixed $\Delta x = \Delta z = 0.042\delta$ but varying Δy_w ($\Delta y_w/h_{\rm wm} = 1.0$, 0.50, 0.33, 0.25, and 0.20). Note that the grids used in this study have uniform spacing Δy_w in the first 5 points near the wall, then a smoothly stretched grid up to $y = 1.4\delta_r$, then uniform spacing $\Delta y_\infty = 0.025\delta_r$ up to $y = 3\delta_r$, and finally smooth stretching up to the top boundary (the only exception is the case with $\Delta y_w/h_{\rm wm} = 1$, where a uniform $\Delta y/h_{\rm wm} = 1$ is used from $y = 0$ to $3\delta_r$). In viscous wall units, $\Delta x^+ = \Delta z^+ \approx 440$ and $h^+_{\rm wm} \approx 590$; hence, the grid spacing is *much* coarser than in traditional wall-resolved LES.

The computed mean velocity is shown in Fig. 1. It is clear that the result for $\Delta y_w/h_{\rm wm} = 1$ (using the wall-model from the first grid point in the traditional manner) yields an overprediction of $U^+_{\rm VD}$. This is trivially connected to the wall stress τ_w through $U^+_{\rm VD} = U_{\rm VD}/\sqrt{\tau_w/\rho_w}$ and further to the skin friction coefficient $C_f = 2\tau_w/(\rho_\infty U^2_\infty)$. An overprediction of $U^+_{\rm VD}$ is, therefore, directly related to an underprediction of τ_w and C_f. On the other hand, by refining Δy_w while keeping $h_{\rm wm}$ fixed, there is clearly a convergence process to the log-law. This confirms the reasoning leading up to criterion (4b). Essentially converged results are obtained for $\Delta y_w/h_{\rm wm} \lesssim 0.5$.

The resolved Reynolds stresses for this test are shown in Fig. 2. The resolved shear stress is directly related to the mean velocity through the stress balance Eq. (2) but brings out the errors a bit more clearly; arguably, $\Delta y_w/h_{\rm wm} \lesssim 0.3$ is needed for grid convergence in this quantity. The

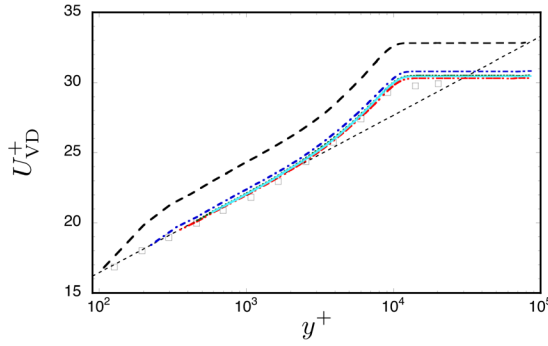

FIG. 5. (Color online) Mean velocity (van Driest-transformed) at $Re_\delta = 6.1 \times 10^5$ ($Re_\theta = 5 \times 10^4$) compared to the log-law $\ln(y^+)/0.41 + 5.2$ (thin dashed line, black) and incompressible experiments at $Re_\theta = 3.1 \times 10^4$ (squares[27]). Fixed grid with $\Delta x/\delta = \Delta z/\delta = 0.042$ and $\Delta y_w/\delta = 0.011$. Varying $h_{\rm wm} = j\Delta y_w$ of 0.011, $j = 1$ (dashed line, black); 0.022, $j = 2$ (dashed-dotted line, blue); 0.033, $j = 3$ (double-dashed double-dotted line, red); 0.044, $j = 4$ (dotted line, green); and 0.055, $j = 5$ (solid line, cyan).

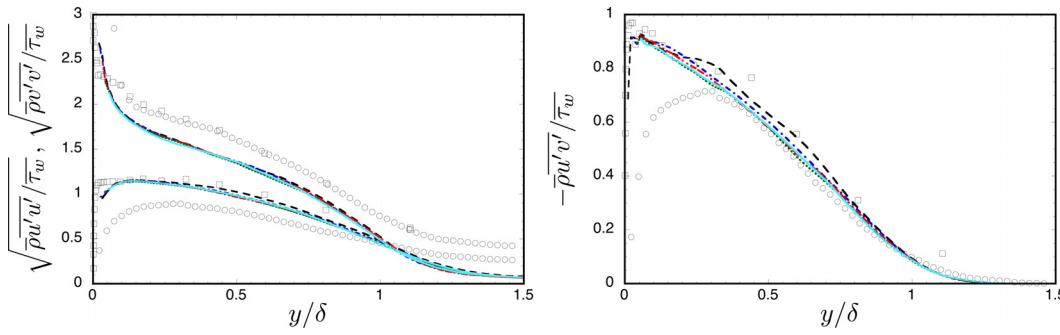

FIG. 6. (Color online) Resolved Reynolds normal stresses (left) and shear stress (right) at $Re_\delta = 6.1 \times 10^5$ ($Re_\theta = 5 \times 10^4$). Fixed grid with $\Delta x/\delta = \Delta z/\delta = 0.042$ and $\Delta y_w/\delta = 0.011$. Varying $h_{\text{wm}} = j\Delta y_w$ as in Fig. 5 compared to corresponding experiments (circles[25,26]) and incompressible experiments at $Re_\theta = 1.3 \times 10^4$ (squares[27]).

normal stresses are less sensitive, with only minor differences during the grid refinement. As discussed in Ref. 26, the underestimation of v' in the corresponding experiments[25,26] is a measurement artifact, related to the dynamic range of the measurement system and the measurement settings. This also leads to an underestimated Reynolds shear stress, particularly below $y/\delta = 0.3$.

The next test investigates criterion (4a) on the wall-parallel grid spacing. In this test, $h_{\text{wm}}/\delta = 0.055$ and $\Delta y_w/h_{\text{wm}} = 0.20$ (i.e., with 5 grid points in the LES below $y = h_{\text{wm}}$) are both fixed while Δx and Δz are varied ($\Delta x/\delta = \Delta\ z/\delta = 0.084$, 0.064, 0.042, and 0.028). The mean velocity and the resolved Reynolds stresses are shown in Figs. 3 and 4. The convergence process is much less clear in this case, suggesting that the wall-parallel grid resolution is less of a factor than the wall-normal one in the numerical and subgrid modeling errors near the wall. Thus, $\Delta x_{1,3}/h_{\text{wm}} \lesssim 0.8$ ($\Delta x/\delta = \Delta z/\delta \lesssim 0.042$) is clearly sufficient for this particular (high-order accurate) numerical method.

The final test is to use a fixed grid (fixed Δx, Δy, and Δz) but with varying h_{wm} ($h_{\text{wm}} = j\Delta y_w$, $j = 1, \ldots, 5$). In this test, $\Delta x = \Delta z = 0.042\delta$, $\Delta y_w = 0.011\delta$. This test mimics the decision one would face in reality: given a fixed grid (related to what is computationally affordable), can the accuracy be improved by increasing h_{wm}? The results of this test are shown in Figs. 5 and 6. Clearly, there is a great improvement in accuracy by abandoning the common practice of using $h_{\text{wm}} = y_1$. For this particular numerical method, it is sufficient to use $h_{\text{wm}} \gtrsim 4\Delta y_w$ (i.e., taking input to the wall-model from the fourth grid point off the wall).

The evolution of the skin friction coefficient $C_{f,\text{inc}}$ is shown in Fig. 7 for the fixed grid with varying $h_{\text{wm}} = j\Delta y_w$, $j = 1, \ldots, 5$. To compare the present compressible flow results with incompressible skin frictions, the van Driest II transformation is used to transform the compressible momentum thickness and skin friction into equivalent incompressible values,[28]

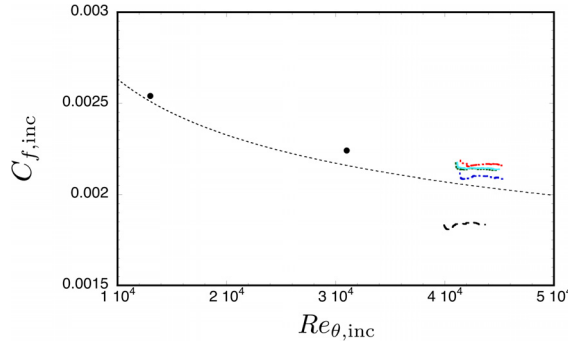

FIG. 7. (Color online) Skin friction evolution as a function of Reynolds number based on momentum thickness for $h_{\text{wm}} = j\Delta y_w$ as in Fig. 5 with fixed grid $\Delta x/\delta = \Delta z/\delta = 0.042$ and $\Delta y_w/\delta = 0.011$ compared to the Kármán-Schoenherr empirical correlation $1/[17.08(\log_{10}Re_{\theta,\text{inc}})^2 + 25.11\log_{10}Re_{\theta,\text{inc}} + 6.012]$ (thin dashed line, black; given in Ref. 29) and incompressible experiments at $Re_\theta = 1.3 \times 10^4$ and 3.1×10^4 (solid circles[27]).

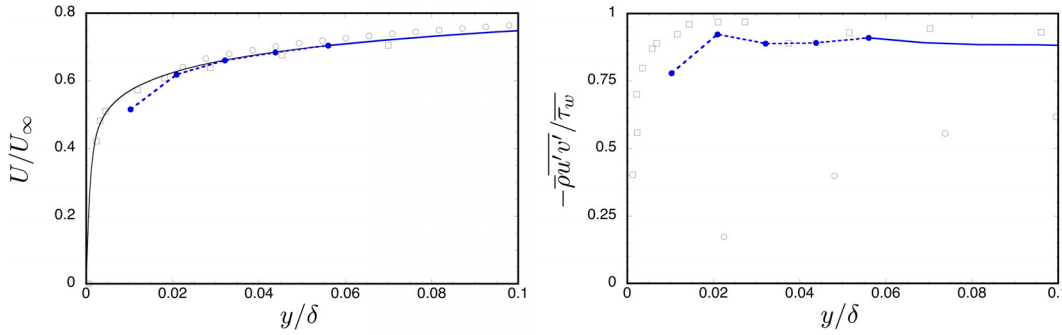

(a)Mean velocity. (b)Reynolds shear stress.

FIG. 8. (Color online) Solution in the LES above (solid line, blue) and below (dashed line with solid circles, blue) the top of the wall-modeling layer at $y = h_{\rm wm} = 0.055\delta$ using $\Delta x/\delta = \Delta z/\delta = 0.042$ and $\Delta y_w/\delta = 0.011$ compared to the mean velocity computed by the wall-model (thin solid line, black, (a) only), corresponding experiments (circles[25,26]), and incompressible experiments at $Re_\theta = 3.1 \times 10^4$ in (a) and $Re_\theta = 1.3 \times 10^4$ in (b) (squares[27]).

$$C_{f,\rm inc} = \frac{\overline{T_w}/T_\infty - 1}{\arcsin^2 \alpha} C_f, \quad \alpha = \frac{\overline{T_w}/T_\infty - 1}{\sqrt{\overline{T_w}/T_\infty \left(\overline{T_w}/T_\infty - 1\right)}}, \quad Re_{\theta,\rm inc} = \frac{\mu_\infty}{\overline{\mu_w}} Re_\theta. \tag{5}$$

With $h_{\rm wm} = \Delta y_w$ (as is used traditionally), the skin friction is clearly underpredicted, but by increasing $h_{\rm wm}$, a much better and grid converged skin friction prediction is achieved. We note that the LES prediction is above the Kármán-Schoenherr empirical correlation given in Ref. 29 by a similar amount as the DeGraaff and Eaton experiments[27] are. The streamwise evolution of C_f also shows how the boundary layer becomes fully developed after an initial adjustment phase; in physical coordinates, this occurs after $x/\delta_r \approx 5$. Note also that the normalization by $\bar{\tau}_w$ used in Fig. 6 (the value of $\bar{\tau}_w$ is different in each case, i.e., $\bar{\tau}_{w,j=1}$ is approximately 15% lower than the $\bar{\tau}_{w,j=5}$) causes the similarity in values between the $h_{\rm wm} = \Delta y_w$ $(j = 1)$ case and the converged results $h_{\rm wm} = j\Delta y_w$, $j \geq 4$; the actual Reynolds stresses obtained by the $h_{\rm wm} = \Delta\, y_w$ case are smaller than the converged results.

Finally, Fig. 8 shows the LES solution above and below $y = h_{\rm wm}$ in the case of $h_{\rm wm} = 0.055$, $j = 5$, together with the solution in the wall-model itself. It is clear that the resolved shear stress is underestimated, and the mean velocity gradient is overpredicted at the first grid point off the wall where the LES is necessarily underresolved (as discussed above). However, the turbulence recovers a realistic and accurate velocity gradient farther away from the wall. The whole point of the proposed approach is to "bypass" this underresolved region, allowing the turbulence to develop before reaching the point where information is fed to the wall-model, thereby ensuring that the wall-model operates with accurate input information from the LES.

These numerical experiments have shown how the computed statistics, especially the so-called "log-layer mismatch" with its associated skin friction error, are improved by abandoning

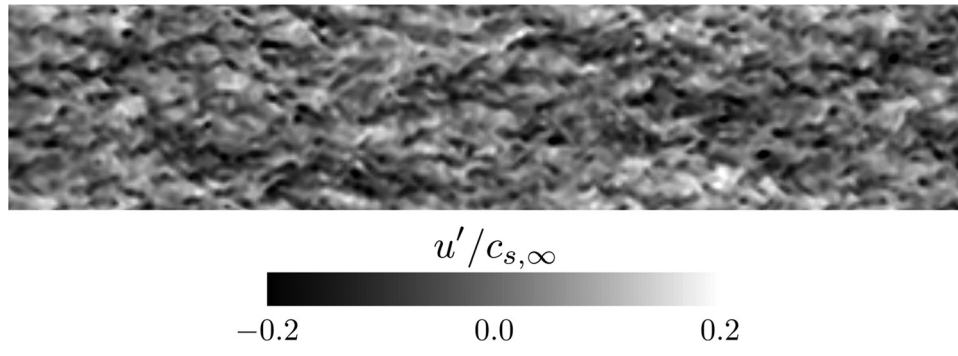

FIG. 9. Instantaneous streamwise velocity fluctuation in a wall-parallel plane $(0 \leq x/\delta_r \leq 15,\ 0 \leq z/\delta_r \leq 3)$ at $y = h_{\rm wm}$ $(h^+_{\rm wm} \approx 590)$ obtained by the case of $h_{\rm wm} = 0.055$, $j = 5$ with $\Delta x/\delta = \Delta z/\delta = 0.042$ and $\Delta y_w/\delta = 0.011$.

the established practice of applying the wall-model at the first grid point off the wall. We finally show contours of the instantaneous streamwise velocity in a wall-parallel plane at the top of the modeled wall-layer (at $h_{wm}^{+} \approx 590$) in Fig. 9. The proposed method (presumably all the methods that model the wall shear stress directly) produces instantaneous turbulence that does not have the "super-streaks" characteristic of many DES or hybrid LES/RANS approaches (cf. Refs. 4 and 5).

IV. CONCLUSIONS

This paper addresses one of the most persistent errors in wall-modeled large eddy simulations: the "log-layer mismatch" with its associated error in the predicted skin friction. The analysis and proposed solution applies to wall-models that directly model the wall stress (so excluding hybrid LES/RANS and DES-type methods). Simple arguments about how the turbulent length scale behaves in the logarithmic layer near a solid wall, coupled with resolution requirements for the numerical method, diagnose the inevitable presence of numerical and subgrid modeling errors in the first few grid points off the wall and yield criteria for the grid resolution that must be satisfied in order for the LES to be well resolved and for the wall-model to receive accurate well-resolved input from the LES. A simple yet very effective method that allows these criteria to be satisfied is proposed: to simply increase the height of the modeled wall-layer while keeping the LES mesh fixed, or, more accurately, to fix the height of the modeled wall-layer while refining the LES mesh until the errors are sufficiently small.

The method (and the thinking behind it) is tested on flat plate boundary layers at $Re_\delta = 6.1 \times 10^5$ ($Re_\theta = 5 \times 10^4$). This Reynolds number is far beyond reach of traditional wall-resolved LES. The method is presented for compressible flow but extends trivially to incompressible flow. Since the crucial point in the proposed method is to feed accurate well-resolved LES information into the wall-model, the method is applicable to any wall-model that estimates the instantaneous wall-stress given instantaneous velocity information (i.e., not only log-law-type models).

ACKNOWLEDGMENTS

The authors gratefully acknowledge Dr. Louis J. Souverein for providing extensive experimental data for validation. The code used in this study is based on an extension to the code FDL3DI provided by Dr. Miguel R. Visbal at the Air Force Research Laboratory. This work was supported in part by the NASA Hypersonics program (Grant NNX08AB30A), the NASA Subsonic Fixed-Wing program (Grant NNX11AI60A), the Air Force turbulence program (Grant FA9550-11-1-0111), and the JAXA International Top Young Fellowship Program. Computer time was provided by the High Performance Computing Center at Stanford University, which is partially funded under the American Recovery and Reinvestment Act of 2009, and by NERSC through successive ERCAP awards.

[1]U. Piomelli and E. Balaras, "Wall-layer models for large-eddy simulations," Annu. Rev. Fluid Mech. **34**, 349 (2002).
[2]P. R. Spalart, "Detached-eddy simulation," Annu. Rev. Fluid Mech. **41**, 181 (2009).
[3]N. V. Nikitin, F. Nicoud, B. Wasistho, K. D. Squires, and P. R. Spalart, "An approach to wall modeling in large-eddy simulations," Phys. Fluids **12**, 1629 (2000).
[4]J. Larsson, F. S. Lien, and E. Yee, "Feedback-controlled forcing in hybrid LES/RANS," Int. J. Comput. Fluid Dyn. **20**, 687 (2006).
[5]U. Piomelli, E. Balaras, H. Pasinato, K. D. Squires, and P. R. Spalart, "The inner-outer layer interface in large-eddy simulations with wall-layer models," Int. J. Heat Fluid Flow **24**, 538 (2003).
[6]M. L. Shur, P. R. Spalart, M. Kh. Strelets, and A. K. Travin, "A hybrid RANS-LES approach with delayed-DES and wall-modelled LES capabilities," Int. J. Heat Fluid Flow **29**, 1638 (2008).
[7]J. E. Brasseur and T. Wei, "Designing large-eddy simulation of the turbulent boundary layer to capture law-of-the-wall scaling," Phys. Fluids **22**, 021303 (2010).
[8]W. Cabot and P. Moin, "Approximate wall boundary conditions in the large-eddy simulation of high Reynolds number flow," Flow, Turbul. Combust. **63**, 269 (1999).
[9]U. Schumann, "Subgrid scale model for finite difference simulations of turbulent flows in plane channels and annuli," J. Comput. Phys. **18**, 376 (1975).
[10]E. Balaras, C. Benocci, and U. Piomelli, "Two-layer approximate boundary conditions for large-eddy simulations," AIAA J. **34**, 1111(1996).
[11]F. Nicoud, J. S. Baggett, P. Moin, and W. Cabot, "Large eddy simulation wall-modeling based on suboptimal control theory and linear stochastic estimation," Phys. Fluids **13**, 2968 (2001).

[12]C. Pantano, D. I. Pullin, P. E. Dimotakis, and G. Matheou, "LES approach for high Reynolds number wall-bounded flows with application to turbulent channel flow," J. Comput. Phys. **227**, 9271 (2008).
[13]P. Moin, K. Squires, W. Cabot, and S. Lee, "A dynamic subgrid-scale model for compressible turbulence and scalar transport," Phys. Fluids A **3**, 2746 (1991).
[14]D. K. Lilly, "A proposed modification of the Germano subgrid-scale closure method," Phys. Fluids A **4**, 633 (1992).
[15]S. K. Lele, "Compact finite difference schemes with spectral-like resolution," J. Comput. Phys. **103**, 16 (1992).
[16]D. V. Gaitonde and M. R. Visbal, "Padé-type higher-order boundary filters for the Navier-Stokes equations," AIAA J. **38**, 2103 (2000).
[17]D. P. Rizzetta, M. R. Visbal, and G. A. Blaisdell, "A time-implicit high-order compact differencing and filtering scheme for large-eddy simulation," Int. J. Numer. Methods Fluids **42**, 665 (2003).
[18]S. Kawai and S. K. Lele, "Localized artificial diffusivity scheme for discontinuity capturing on curvilinear meshes," J. Comput. Phys. **227**, 9498 (2008).
[19]S. Kawai, S. K. Shankar, and S. K. Lele, "Assessment of localized artificial diffusivity scheme for large-eddy simulation of compressible turbulent flows," J. Comput. Phys. **229**, 1739 (2010).
[20]S. Kawai and S. K. Lele, "Large-eddy simulation of jet mixing in supersonic crossflows," AIAA J. **48**, 2063 (2010).
[21]G. Urbin and D. Knight, "Large-eddy simulation of a supersonic boundary layer using an unstructured grid," AIAA J. **39**, 1288 (2001).
[22]B. Morgan, J. Larsson, S. Kawai, and S. K. Lele, "Improving the low-frequency characteristics of recycling/rescaling inflow turbulence generation," AIAA J. **49**, 582 (2011).
[23]S. B. Pope, *Turbulent Flows* (Cambridge University Press, UK, 2000).
[24]S. T. Bose, P. Moin, and D. You, "Grid-independent large-eddy simulation using explicit filtering," Phys. Fluids **22**, 105103 (2010).
[25]L. J. Souverein, P. Dupont, J. F. Debieve, J. P. Dussauge, B. W. van Oudheusden, and F. Scarano, "Effect of interaction strength on unsteadiness in turbulent shock-wave-induced separations," AIAA J. **48**, 1480 (2010).
[26]L. J. Souverein, "On the scaling and unsteadiness of shock induced separation," Ph.D. dissertation (Delft University of Technology, 2010).
[27]D. B. DeGraaff and J. K. Eaton, "Reynolds-number scaling of the flat-plate turbulent boundary layer," J. Fluid Mech. **422**, 319 (2000).
[28]S. Pirozzoli, F. Grasso, and T. B. Gatski, "Direct numerical simulation and analysis of a spatially evolving supersonic turbulent boundary layer at $M = 2.25$," Phys. Fluids **16**, 530 (2004).
[29]E. J. Hopkins and M. Inouye, "An evaluation of theories for predicting turbulent skin friction and heat transfer on flat plates at supersonic and hypersonic mach numbers," AIAA J. **9**, 993 (1971).